EUROPEAN ORGANIZATION FOR NUCLEAR RESEARCH

CERN-EP/87-213
25 November 1987

LIGHT NUCLEUS PRODUCTION IN $\bar{p}^4$He ANNIHILATION BETWEEN 0 AND 600 MeV/c

F. Balestra, S. Bossolasco, M.P. Bussa, L. Busso, L. Fava, L. Ferrero,
D. Panzieri, G. Piragino and F. Tosello,
Istituto di Fisica Generale 'A. Avogadro', University of Turin and
INFN, Sezione di Torino, Turin, Italy

R. Barbieri, G. Bendiscioli, R. Rotondi, P. Salvini and A. Zenoni,
Dipartimento di Fisica Nucleare e Teorica, University of Pavia and INFN, Sezione di Pavia, Italy

Yu.A. Batusov, I.V. Falomkin, F. Nichitiu, G.B. Pontecorvo, M.G. Sapozhnikov and V.I. Tretyak,
Joint Institute for Nuclear Research, Dubna, USSR

C. Guaraldo and A. Maggiora,
Laboratori Nazionali di Frascati dell'INFN, Frascati, Italy

E. Lodi Rizzini,
Dipartimento di Automazione Industriale, University of Brescia and INFN, Sezione di Pavia, Italy

A. Haatuft, A. Halsteinslid, K. Myklebost and J.M. Olsen,
Physics Department, University of Bergen, Norway

F.O. Breivik, T. Jacobsen and S.O. Sørensen,
Physics Department, University of Oslo, Norway

ABSTRACT

The production rate of ^{3}H is deduced in an approximate way from that of ^{3}He, and the lower and upper limits for the production rate of p and ^{2}H in $\bar{p}^4$He annihilation between 0 and 600 MeV/c are measured. The momentum distributions for the different particles are given.

(Submitted to Nuovo Cimento)

1. Introduction

In previous papers [1-5] we reported a number of experimental data on the $\bar{p}^{4}He$ interaction between 0 and 600 MeV/c obtained with a self-shunted streamer chamber in a magnetic field [6] at the LEAR facility of CERN. In particular, we gave the cross sections for the reaction ($\bar{p}^{4}He$ -> ^{3}He + anything) at 192.8±1.0, 306.2±1.8 and 607.7±1.4 MeV/c (19.6, 48.7 and 179.6 MeV, respectively) and its branching ratio for $\bar{p}$ at rest.

In this paper we contribute to this field with measurements of the production of proton (p), deuterons (^{2}H) and tritons (^{3}H) both at rest and at the above energies and of the momentum distributions of all the mentioned particles. In addition, we summarize the results obtained in the preceding papers concerning the reaction cross sections for some $\bar{p}$ ^{4}He reaction channels, the total charged prong multiplicity distributions and the negative pion multiplicity distributions. Some results are given with a higher statistics than in the previous papers.

This information is of particular interest in cosmological problems, as stressed in Refs. 7. Moreover, it may help to understand the annihilation mechanism in nuclear matter [8,9], the nuclear structure [10] and the $\bar{p}$-nucleon interaction [11].

While interacting with ^{4}He nuclei, $\bar{p}$ undergo elastic and non-elastic interactions. Above about 24 MeV the non elastic interaction includes $\bar{p}p$ charge exchange, break up and annihilation processes; below 24 MeV, only annihilation is effective [2]. The annihilation is by far the strongest non elastic interaction; charge exchange contributes about 2% only [3], and the other reactions about 6% [4]. The

final products of the annihilation events are mesons (mostly pions (π)), neutrons (n), p, ^{2}H and ^{3}H.

We shall call any process which precedes the annihilation, such as $\bar{p}p$ charge exchange and break up reactions an initial state interaction (ISI). We shall call any process which follows the annihilation, such as pion-nucleon and nucleon-nucleon interactions a final state interaction (FSI). ISI and FSI provoke the desappearance of ^{3}H and ^{3}He from the final particles.

As it was discussed in detail in Ref. [3], in the annihilation events the type and the number of heavy particles in the final state and the number of charged prongs are related as shown in Tab. I. (A) represents annihilation on neutrons; (B) are annihilations on p; (C) are annihilation on p followed by ($\pi p \rightarrow \pi^0 n$) charge exchange or ($\pi(pn) \rightarrow nn$) absorption interactions leading to all neutral heavy particles (neutrons) in the final state); (D) are mainly annihilations on p preceded by ISI or followed by FSI with break of the ^{3}H nuclei; (E) are mainly annihilations on n preceded by ISI or followed by FSI with disintegration of the ^{3}He nuclei.

We note that pion-nucleon charge exchange transforms events of type (D) into events of type (E) and viceversa, but the operation is almost in balance so that the numbers of events of type (D) and (E) are substantially unchanged (for a discussion on this point see Refs. [3,5]). Hence the main effect of FSI is the break up of ^{3}H and ^{3}He nuclei into ^{2}H, p and n.

Above 24 MeV, the $\bar{p}p - \bar{n}n$ charge exchange interaction not followed by annihilation contributes to the events with one heavy

prong; the break-up interaction not followed by annihilation contributes to the events with 2 and 3 charged prongs.

2. ^{3}H production.

We recall that (i) ^{3}He is produced only in even prong events, (ii) p, ^{2}H and ^{3}H are produced only in odd prong events and (iii) odd prong events with two heavy prongs arise from $\bar{p}n$ annihilations (neglecting charge exchange effects). These features allowed us [3] to measure the cross section for the production of ^{3}He and for the annihilation of $\bar{p}$ on p and on n bound in the ^{4}He structure, which are reported in Tab. II, together with other quantities useful in the following.

We notice that there are some differences between the values of the cross sections and of the percentages at rest and at 607 MeV/c given in Ref. [3] and in Tab. II. The new values are more reliable because a higher statistics was used and the break up events were separated from the annihilation ones at 607 MeV/c [4].

Starting from these data, we shall now calculate in an approximate way the production of ^{3}H.

The percentage of events with annihilation on n and break up of the ^{3}He structure is

$$P(^3\text{He break}) = P(\bar{p}n) - P(^3\text{He}) = P(\bar{p}n) - P_e \qquad (1)$$

where $P(\bar{p}n)$ is the percentage of annihilations on n bound in the ^{4}He structure and $P_e = P(^3\text{He})$ is the percentage of even prong events.

Similarly, for the case of $\bar{p}p$ annihilation events, we write

$$P(^3H \text{ break}) = P(\bar{p}p) - P(^3H) \tag{2}$$

where $P(\bar{p}p)$ refers to annihilation on p bound in the ^4He nucleus. Now we assume

$$\frac{P(^3H \text{ break})}{P(^3He \text{ break})} = \frac{P(\bar{p}p)}{P(\bar{p}n)} = \frac{1}{R} \tag{3}$$

so that

$$P(^3H) = P(^3He)/R \tag{4}$$

As a partial justification of eq.(4), let us suppose that the only process which breaks ^3H and ^3He is FSI involving pions. We can define the probability of FSI with break up of ^3H and ^3He by the equations

$$P_{FSI}(^3He) = \frac{P(\bar{p}n) - P_e}{P(\bar{p}n)} \tag{5}$$

$$P_{FSI}(^3H) = \frac{P(\bar{p}p) - P(^3H)}{P(\bar{p}p)} \tag{6}$$

and assume

$$\frac{P_{FSI}(^3H)}{P_{FSI}(^3He)} = \frac{\sigma^T_{FSI}(^3H)}{\sigma^T_{FSI}(^3He)} = R_{FSI} \tag{7}$$

where $\sigma_{FSI}(^3H)$ is the total cross section for the interaction of the ^3H nucleus with the pions produced in the $\bar{p}n$ annihilations and $\sigma_{FSI}(^3He)$ has the same meaning for ^3He. Combining eqs. (5), (6) and (7),

one obtains

$$P(^3H) = P(\bar{p}p)\,(1 - R_{FSI}(1 - P_e/P(\bar{p}n))) \qquad (8)$$

The values of P_e, $P(\bar{p}p)$ and $P(\bar{p}n)$ are given in Tab. II, while the value of R_{FSI} can be estimated in an approximate way as follows.

In the $\bar{p}p$ annihilation the residual nucleons are (p + 2n) and, on the average, the number of pions produced is $(1.5\pi^+ + 1.5\pi^- + 2\pi^\circ)$[12]. In the $\bar{p}n$ annihilation the residual nucleons are (n + 2p) and the pions are $(1\pi^+ + 2\pi^- + 2\pi^\circ)$[12]. The pion momenta are in the region of the baryonic resonance momentum (~ 300 MeV/c) [13,14], so the cross sections for the different pion-nucleon pairs are approximately in the ratio [14]

$$\sigma(\pi^+p) : \sigma(\pi^\circ p) : \sigma(\pi^-p) : \sigma_{ce} = 9:4:1:2$$

Therefore, considering the possible pion-nucleon pairs, one obtains

$$R_{FSI} = 1.034$$

As R_{FSI} is close to 1, eq. (8) practically coincides with eq. (4). Eq. [4] gives for $P(^3H)$ the values reported in Tab. II, Fig. 1 and Fig. 2.

3. p and ^2H production.

For the production of p and ^2H we can give only upper and lower limits. The lower limit for a given particle is obtained from the percentage of events in which this particles is recognized; the upper limit is obtained from the percentage of events from which the presen-

ce of the same particle is excluded. To this end, we have proceeded as follows.

First, we observe that the upper limits for the percentage of events, where no ^3H neither ^3He are produced (i.e., only pions, or p, or ^2H, are produced), is

$$P\ (0,p,^2H) = 1 - (P(^3He) + P\ (^3H)) \qquad (5)$$

0 means no heavy particles (only pions).

Second, protons are produced in all the events with 2 heavy prongs, the percentage of which (P(2h)) was measured and is reported in Tab. II. Third, following the criteria described in Ref. [15], we measured a sample of events and in part of them recognized the type of heavy particle produced. Also, we measured the total charged prong multiplicity distributions (pions plus heavy prongs) of the odd prong events with ≤ 1 heavy prongs (M_{1i}) and with 2 heavy prongs (M_{2i}), (ΣM_{2i} = P(2h)).

We calculated the lower limits for the production of no heavy prong events, of p or of ^2H, by the relations:

$$\begin{aligned} P_l(0) &= \Sigma\ M_{1i}\ N_{1i}(0)/N_{1i} \\ P_l(p) &= \Sigma\ M_{1i}\ N_{1i}(p)/N_{1i} + P(2h) \\ P_l(^2H) &= \Sigma\ M_{1i}\ N_{1i}(^2H)/N_{1i} + \Sigma\ M_{2i}\ N_{2i}(p^2H)/N_{2i} \end{aligned} \qquad (6)$$

where $N_{1i}\ (x)$ is the number of ≤ 1 heavy prong events of multiplicity i in which the particle x was recognized, N_{1i} is the corresponding total number of measured events, $N_{2i}(p^2H)$ is the number of two prong events of multiplicity i where a deuteron was identified and N_{2i} is the corresponding total number of measured events; i is an odd number

going from 1 to 9. The weights M_{1i} and M_{2i} were measured firstly in Ref. [3], but for the present work a higher statistics was used. They were introduced in the preceding relations according to Ref. [3] to compensate for some inefficiency in recognizing ≤ 1 heavy prong events and two prong events.

The upper limits for the different particle production are given by the relations:

$$P_u(0) = (1 - P(^3H) - P(^3He)) - P_1(p) - P_1(^2H) + \Sigma M_{2i}N_{2i}(p^2H)/N_{2i} \quad (7)$$

$$P_u(p) = (1 - P(^3H) - P(^3He)) - P_1(0) - \Sigma M_{1i}N_{1i}(^2H)/N_{2i} =$$
$$= (1 - P(^3H) - P(^3He)) - P_1(0) - P_1(^2H) + \Sigma M_{2i}N_{2i}(p^2H)/N_{2i}$$

$$P_u(^2H) = (1 - P(^3H) - P(^3He)) - P_1(0) - P_1(p) + (P(2h) - P(2p))$$

where P(2p) is the percentage of events in which 2 protons were recognized.

We measured the upper and lower limits for $\bar{p}$ at rest, at 306.2 MeV/c and at 607.7 MeV/c and the behaviour vs. $\bar{p}$ momentum of the probability intervals is sketched in Fig. 3. 644 events with $\bar{p}$ at rest and 459 at 607.7 Mev/c were utilized; the numbers of odd prong events where it was possible to recognize the presence of ≤ 1 heavy prongs or 2 heavy prongs were 231 and 184 at the two energies, respectively.

We stress that the whole percentage of events without heavy prongs or with p or ^2H cannot exceed $(1 - P(^3He) - P(^3H))$. Of course, $P_u(0) + P_u(p) + P_u(^2H) > P(0,p,^2H)$ due to the normalization, because

sometimes, in P(2h) cases, p and ^2H (or 2p) may occur in the same event.

Moreover, we note that above 24 MeV there is a small contribution to the $\bar{p}^4He$ interaction arising from the $\bar{p}p \rightarrow \bar{n}n$ charge exchange interaction and from the break-up interaction. The latter one contributes to the ^3He production with 4.2 mb[4], 1.9% of the annihilation cross section; both processes contribute to the ^3H production with more than about 5 mb, i. e. 2.3% of the annihilation cross section.

4. Comments

One sees that

a) the production of ^3H is higher than that of ^3He. This is a consequence of the fact that $\sigma^a(\bar{p}p)$ is higher than $\sigma^a(\bar{p}n)$ (see Tab. II and Ref. [3]).

b) the productions of ^3He and ^2H have the same magnitude with an increase of that of ^2H and a decrease of that of ^3He as the $\bar{p}$ momentum increases. This result contradicts the prediction of Ref. [10], which indicates a ^2H production four times higher than that of ^3He. Moreover, the cross section for the production of ^3He found by us is higher by a factor of 1.5-1.8 than that predicted by ref. [10].

5. Momentum distributions of the heavy particles.

The momentum was measured following the criteria described in Ref. [15] based on the measurement of coordinates on stereoscopic plane projections and on the spatial reconstruction of tracks by means

of CERN geometry programs.

The ^{4}He gas target was at atmospheric pressure and the values of the magnetic field for the different $\bar{p}$ momenta were: at rest 2.3 T (for part of the events 4.1 T), at 200 MeV/c 4.2 T, at 300 MeV/c 6.2 T and at 600 MeV/c 8.1 T. The shortest tracks of the stopping ^{3}He nuclei were about 1cm in length.

As we have already stressed, ^{3}He nuclei are the only heavy particles produced in the even-prong events and, owing to high ionization, their tracks are not confused with those of positive pions. Hence their momentum distributions at different $\bar{p}$ momenta are not affected by confusion with other particles.

In the case of odd prong events, the heavy particles may be p, ^{2}H or ^{3}H and recognition was performed on the basis of information such as the geometric form of the track, the track luminosity, the streamer density and the baryon and the electric charge conservation laws, as described in Ref. [15]. The prong analysis led to three different situations: (i) the particle is identified as p, ^{2}H or ^{3}H; (ii) it is not possible to distinguish among p, d and ^{2}H, but the pion mass is excluded; (iii) it is not possible to recognize the mass at all, i.e. it may be that of p, d, t or pion.

The momentum distributions for the different cases are shown in Figs. 4 a, b, c, d and 5 a, b; for the identified masses, some values of the kinetic energy are reported on the abscissae too. Since, within the limits of our statistics, no dependence on the $\bar{p}$ momentum appears, for each particle we summed up into a sole histogram the momentum distributions at different $\bar{p}$ momenta. The direction of most of the identified prongs is within $\pm$ 30° with respect to a plane perpendicular to the magnetic field direction. This favours good stereoscopic

view and good precision in the curvature measurement. Typical relative errors (mean values) of the momenta of the identified particles for $\bar{p}$ at rest and at 607 MeV/c are: for ^{3}He, 14.4% and 2.3%; for p, 13.7% and 9.9%; for π^-, 19.3% and 10.0%, respectively. As expected, the errors increase as the magnetic field decreases (from 8.1T down to 2.3T).

The momentum distributions for ^{2}H, ^{3}H and ^{3}He extend mostly below 500 MeV/c, with a maximum for ^{3}H and ^{3}He around 130 MeV/c (4 MeV). The mean value of the ^{3}He momentum is 198.±9. The momentum distribution of p extends up to 600 MeV/c with a large maximum around 160 MeV/c (12.5 MeV). Combining these distributions one obtains a distribution like that of Fig. 5a. We stress again that only the ^{3}He momentum distribution is not affected by the inefficiency in mass identification.

Presumably, the momentum distribution of the protons extends above 600 MeV/c, but at these high momenta protons and pions produce nearly the same ionization and are not distinguishable. In fact, the momentum distribution of the unidentified positive particles (heavy particles plus mesons) extends above 600 MeV/c (Fig. 5b) and the comparison between the momentum distributions of the negative and the identified positive mesons points to a lack of positive mesons with high momentum.

For comparison, we report also (see Fig. 6 and 7) the momentum distributions at rest and at 600 MeV/c of the π^- produced in all the events and that of the $\pi^\pm$ in the events with production of ^{3}He. These distributions are not affected by the presence of the momenta of other particles. For the case of $\bar{p}$ at rest (low value of the magnetic field), only tracks within $\pm$ 30° with respect to a plane perpendicular

to the magnetic field direction were selected. The π^- distribution at rest is compared with the same distribution for the annihilation $\bar{p}n \to \pi^-$ + anything in deuterium [13] and the distribution at 600 MeV/c is compared with the π^- distribution for $\bar{p}p$ annihilation in hydrogen at 700 MeV/c [13].

One sees that the π^- and $\pi^\pm$ distributions from ^{4}He are richer in lower momenta than that from deuterium. This is due mainly to the FSI which allows transfer of momentum from the annihilation pions to the recoil nuclei (^{3}H or ^{3}He), that may break into nucleons. The percentage of π-nucleon FSI with break up of ^{3}H and ^{3}He is given at most by $(1-P(^3H)-P(^3He))$, and the values are listed in Tab.2.

In spite of the impossibility of identifying all the positive particles, it is possible to calculate the mean numbers per event of heavy charged prongs and of positive mesons. Indeed, neglecting πN charge exchange effects, the mean number per event of heavy charged prongs is given by the formula:

$$\langle n_h \rangle = 1 \times P(1h) + 2 \times P(2h) =$$
$$= 1 \times (P(\bar{p}p) + P(^3He)) + 2 \times P(2h)$$

and the mean number of π^+ per event is given by:

$$\langle n_{\pi^+} \rangle = \langle n_c \rangle - \langle n_{\pi^-} \rangle - \langle n_h \rangle$$

where $\langle n_c \rangle$ is the mean number of charged prong per event and $\langle n_{\pi^-} \rangle$ is the mean number of π^-. $\langle n_c \rangle$ and $\langle n_{\pi^-} \rangle$ are known experimentally from the charged prong multiplicity distributions (see Refs. [2,3] and fig.8) and are reported in Tab. III, together with the calculated values of $\langle n_h \rangle$ and $\langle n_{\pi^+} \rangle$. Due to the occurrence of events without heavy prongs (see Fig. 3), $\langle n_h \rangle$ is overestimated (5-10%), so that the values of $\langle n_{\pi^+} \rangle$ are underestimated, accordingly.

From the above mean values and the numbers of identified $\pi^\pm$ and

heavy prongs, we estimated that both π^+ and heavy particles contribute about 50% each to the momentum distribution of the unidentified particles. We note that the values of $\langle n_{\pi^-} \rangle$ and $\langle n_{\pi^+} \rangle$ and of ratio $\langle n_{\pi^+} \rangle / \langle n_{\pi^-} \rangle$ are close to those found for the $\bar{p}$ annihilation in deuterium [12] and carbon [16] and higher than those found for Ag and Br in photographic emulsions [17].

6. Conclusions

The production of ^3H in the annihilation of $\bar{p}$ on ^4He at rest and at 192.8, 306.2 and 607.7 Mev/c was deduced in an approximate way from the measured production of ^3He. Lower and upper limits for the production of p and ^2H and for the $\bar{p}p$ annihilation followed by ($\pi^- p \rightarrow \pi^0 n$) charge exchange or ($\pi^-(pn) \rightarrow nn$) absorption were measured. The results are shown in Tab. II and Figs. 2 and 3. The production of ^3H is higher than that of ^3He and both decrease with the $\bar{p}$ momentum, so that the production of other particles increases accordingly. The production of ^2H is of the same order of magnitude as that of ^3He. The results on ^2H and ^3He disagree strongly with the theoretical predictions of Ref. [10].

The momentum distributions of p, ^2H, ^3H, ^3He were measured too (see Figs.4 and 5). Within the limits of our statistics, for each particle, the momentum distribution does not depend on the $\bar{p}$ momentum. The ^3H and ^3He distributions have maxima around 130 Mev/c (4 MeV), while the π momentum distributions exhibit maxima around 180 MeV/c. The latter ones are richer in lower momenta than the momentum distributions of the pions produced in annihilation on hydrogen and deuterium.

References

1 - F.Balestra, Yu.A.Batusov, G.Bendiscioli, M.P.Bussa, L.Busso, I.V.Falomkin, L.Ferrero, V.Filippini, G.Fumagalli, G.Gervino, C.Guaraldo, E.Lodi Rizzini, A.Maggiora, D.Panzieri, G.Piragino, G.B.Pontecorvo, A.Rotondi, M.G.Sapozhnikov, F.Tosello, M.Vascon, A.Venaglioni, G.Zanella, A.Zenoni: Phys. Lett. 149B, 69 (1984)

2 - F.Balestra, M.P.Bussa, L.Busso, L.Ferrero, D.Panzieri, G.Piragino, F.Tosello, C.Guaraldo, A.Maggiora, Yu.Batusov, I.V.Falomkin, G.B.Pontecorvo, M.G.Sapozhnikov, G.Bendiscioli, V.Filippini, G.Fumagalli, C.Marciano, R.Rotondi, A.Zenoni, E.Lodi Rizzini, M.Vascon, G.Zanella: Phys. Lett. B165, 265 (1985)

3 - F.Balestra, S.Bossolasco, M.P.Bussa, L.Ferrero, D.Panzieri, G.Piragino, F.Tosello, G.Bendiscioli, A.Rotondi, P.Salvini, A.Zenoni, S.Guaraldo, A.Maggiora, Yu.Batusov, I.V.Falomkin, F.Nichitiu, G.B.Pontecorvo, M.G.Sapozhnikov, E.Lodi Rizzini: Nucl. Phys. A465, 714 (1987)

4 - F.Balestra, R.Barbieri, Yu.A.Batusov, G.Bendiscioli, S.Bossolasco, M.P.Bussa, L.Busso, I.V.Falomkin, L.Ferrero, C.Guaraldo, L.A.Kondratyuk. E.Lodi Rizzini, A.Maggiora, F.Nichitiu, D.Panzieri, G.Piragino, G.B.Pontecorvo, A.Rotondi, P.Salvini, M.G.Sapozhnikov, F.Tosello, A.Zenoni: Phys. Lett. B194, 343 (1987)

5 - F.Balestra, S.Bossolasco, M.P.Bussa, L.Busso, L.Fava, L.Ferrero, D.Panzieri, G.Piragino, F.Tosello, G.Bendiscioli, R.Rotondi, P.Salvini, A.Zenoni, Yu.A.Batusov, S.A.Bunyatov, I.V.Falomkin, F.Nichitiu, G.B.Pontecorvo, M.G.Sapozhnikov, V.I.Tretyak, C.Guaraldo, A.Maggiora, E.Lodi Rizzini, A.Haatuft, A.Halsteinslid, K.Myklebost, J.M.Olsen, F.O.Breivik, T.Jacobsen, S.O.Sørensen: CERN-EP/87-65; in press on Nuovo Cimento.

6 - F.Balestra, M.P.Bussa, L.Busso, L.Ferrero, G.Gervino, A.Grasso, D.Panzieri, G.Piragino, F.Tosello, G.Bendiscioli, V.Filippini, G.Fumagalli, E.Lodi Rizzini, C.Marciano, A.Rotondi, A.Venaglioni, A.Zenoni, C.Guaraldo, A.Maggiora, A.Cavestro, M.Vascon, G.Zanella, Yu.K.Akimov, Yu.A.Batusov, I.V.Falomkin, G.B.Pontecorvo: Nucl. Instr. Meth., A234, 30 (1985)

7 - Ya. B. Zeldovich, M.Yu Khlopov, V.M.Chechetkin and M.G.Sapzhnikov: Phys. Lett. 118B, 329 (1982)
- V.M. Chechetkin, M.Yu Khlopov and M.G. Sapozhnikov: Riv. Nuovo Cimento 5,1 (1982)
- M.Yu.Khlopov, A.D.Linde: Phys. Lett. 138B, 265 (1984)
- J.Ellis, D.V.Nanopoulos, S.Sarkar: Nucl. Phys. B259, 175 (1985)
- R.Dominguez Tenreiro, G.Yepes: FTUAM-86/13 (Madrid)
- Yu.A.Batusov, I.V.Falomkin, G.B.Pontecorvo, M.G.Sapozhnikov, C.Guaraldo, A.Maggiora, M.Vascon, G.Zanella, G.Bendiscioli, V.Filippini, E.Lodi Rizzini, A.Rotondi, A.Zenoni, F.Balestra, M.P.Bussa, L.Busso, L.Ferrero, G.Gervino, D.Panzieri, G.Piragino, F.To-

sello: Lettere al Nuovo Cimento 41, 223 (1984)
- Yu.A.Batusov, S.A.Bunyatov, I.V.Falomkin; F.Nichitiu, B.Pontecorvo; M.G.Sapozhnikov, C.Guaraldo; A.Maggiora; M.Vascon, G.Zanella, G.Bendiscioli, V.Filippini, E.Lodi Rizzini, A.Rotondi, A.Zenoni, F.Balestra, M.P.Bussa, L.Busso; L.Ferraro, G.Gervino, D.Panzieri, G.Piragino, F.Tosello, M.Yu.Khlopov: JINR Rapid Communications 6-85

8 - M.R.Clover, R.M.DeVries, N.J.DiGiacomo, Y.Yariv: Phys. Rev. C26, 2138 (1982)
- P.L.McGaughey, M.R.Clover, N.J.DiGiacomo: Phys. Lett. 166B, 264 (1986)
- M.Cahay, J.Cugnon, J.Vandermeulen: Nucl. Phys. A393, 237 (1983)
- J.Cugnon, J.Vandermeulen: Nucl. Phys. A445, 717 (1985)
- A.S.Iljinov; V.I.Nazaruk, S.E.Chigrinov: Nucl. Phys. A382, 378 (1982)
- S.C.Phatak, N.Sarma: Unpublished
- E.Hernandez, E.Oset: Nucl. Phys. A455, 584 (1986)

9 - P.L.McGaughey, K.D.Bol, M.R.Clover, R.M.DeVries, N.J.DiGiacomo, J.S.Kapustinsky, W.E.Sondheim, G.R.Smith; J.W.Sunier; Y.Yariv, M.Buenerd, J.Chauvin; D.Lebrun, P.Martin, J.C.Dousse: Phys. Rev. Lett. 20, 2156 (1986)
- P.L.McGaughey, N.J.DiGiacomo, W.E.Sondheim, J.W.Sunier, Y.Yariv: Nucl. Instr. Meth. A249, 361 (1986)
- E.F.Moser, H.Daniel, T.Von Egidy, F.J.Hartmann, W.Kanert, G.Schmidt, M.Nicholas, J.J.Reidy: Phys. Lett. B179, 25 (1986)
- F.Balestra, S.Bossolasco; M.P.Bussa, L.Busso; L.Ferrero, A.Grasso, D.Panzieri, G.Piragino, T.Tosello, G.Bendiscioli, V.Filippini, G.Fumagalli, C.Marciano, A.Rotondi, A.Zenoni, C.Guaraldo, A.Maggiora, Yu.A.Batusov, I.V.Falomkin, G.B.Pontecorvo, M.G.Sapozhnikov, M.Vascon, G.Zanella; E.Lodi Rizzini: Nucl. Phys. A452, 373 (1986)
- Yu.A.Batusov, S.A.Bunyatov, I.V.Falomkin, G.B.Pontecorvo, M.G.Sapozhnikov, F.Balestra, S.Bossolasco, M.P.Bussa, L.Busso, L.Ferrero, D.Panzieri, G.Piragino, F.Tosello, C.Guaraldo, A.Maggiora, G.Bendiscioli, V.Filippini, A.Rotondi, A.Zenoni, E.Lodi Rizzini: Europhys. Lett. 2; 115 (1986)
- F.O.Breivik, T.Jacobsen; S.O.Sørensen: Phys. Scr. 28, 862 (1983) and Report 84-15, Inst. of Phys. (Oslo, 1984)

10 - V.I.Nazaruk: Phys. Lett. 155B, 323 (1985)

11 - L.A.Kondratyuk, M.Zh.Shmatikov: Phys. Lett. 117B, 381 (1982)
- I.Grach, M.Shmatikov: ITEP-12 (Moscow, 1982) and ITEP-10 (Moscow, 1982)

12 - R.Bizzarri, P.Guidoni, F.Marcelja, F.Marzano, E.Costelli, M.Sessa: Nuovo Cimento A22, 225 (1974)
- T.Kalogeropoulos, G.S.Tzanakos: Phys. Rev., D22, 2585 (1980)
- R.Armenteros, B.French: High Energy Phys.; vol. 4 (New York, N.Y., 1969)
- U.Amaldi jr., B.Conforto, G.Fidecaro, H.Steiner, G.Baroni, R.Bizzarri, P.Guidoni, V.Rossi; G.Brautti; E.Castelli, M.Ceschia, L.Chersovani, M.Sessa: Nuovo Cimento 46A, 171 (1966)

13 - J.Roy: $\bar{p}d$ annihilation at rest. 4th Int. Symp. on $\bar{N}N$ interaction, Syracuse (1975), pag.III 1.
- S.Saito, Y.Hattari, J.H.Kim, T.Yamageta: Inst. Phys. Conf. Ser. N. 73: Section 8 VII Eur. Symp. Antiproton Interactions, Durham 1984; pg 519

14 - B.H.Brandsen, R.G.Moorhouse: The pion-nucleon system. Princeton University Press (1973)

15 - F.Balestra, M.P.Bussa, L.Busso, L.Fava, L.Ferrero, D.Panzieri, G.Piragino, F.Tosello, G.Bendiscioli, G.Fumagalli, A.Rotondi, P.Salvini, A.Zenoni, C.Guaraldo, A.Maggiora, Yu.A.Batusov, I.V.Falomkin, G.B.Pontecorvo, M.G.Sapozhnikov, E.Lodi Rizzini: Nucl. Instr. Meth. A257, 114 (1987)

16 - L.E.Agnew, Jr.,T.Elioff, W.B.Fowler, R.L.Lander, W.M.Powell, E.Segre', H.M.Steiner, H.S.White, C.Wiegand; T.Ypsilantis: Phys. Rev. 118, 1371 (1960)

17 - A.G.Ekspong, A.Frisk, S.Nilsson, B.E.Ronne: Nucl. Phys. 22, 353 (1961)

Table captions

Tab. I Number and type of the heavy charged particles produced in the $\bar{p}^4$He annihilation. See text for the meaning of (A), (B), etc.

Tab. II Cross sections (σ, mb) and branching ratios (P, %) for different processes occurring in the $\bar{p}^4$He interaction at four $\bar{p}$ momenta. σ_R = reaction cross section including all the non elastic processes; σ_{CE} = $\bar{p}p \rightarrow \bar{n}n$ charge exchange cross section; σ_{BU} = break up cross section with production of 2 and 3 heavy prongs; σ_a = annihilation cross section. $\sigma_a(^3He)$ = cross section for the annihilation with production of ^{3}He nuclei. $P(^3He)$ = percentage of annihilations with production of ^{3}He ($P(^3He) = \sigma_a(^3He)/\sigma_a$); P_o = percentage of annihilations with production of an odd number of charged prongs; $P(\bar{p}p)$ = percentage of $\bar{p}p$ annihilations; $P(\bar{p}n)$ = percentage of $\bar{p}n$ annihilations; P(2h) = percentage of annihilations with production of 2 heavy prongs. $P(^3H)$ = percentage of annihilations with production of ^{3}H nuclei; $\sigma(^3H)$ = cross section for the annihilation with production of ^{3}H; $P(0, p, ^2H) = 1 - P(^3He) - P(^3H)$ = percentage of events with production of particles other than ^{3}H and ^{3}He. The last three lines display some final results of this work.

The other data at rest are like those of Ref. [3], but were obtained with a higher statistics; the data at 192.8 MeV/c and at 306.2 MeV/c are taken from Ref. [3]; the data at 607.7 MeV/c are like those of Ref. [3] but here the annihilation events are separated from the break-up and the charge

exchange ones, and a higher statistics was used. The break-up data are taken from Ref. [4]. The charge exchange cross section was evaluated to be about 2% of the reaction cross section (Ref. [3]).

At 306.2 MeV/c the break-up events are confused with the annihilations (σ_a includes σ_{BU}); σ_{CE} has been estimated; non annihilation events should be less than 10% (see data at 607.7 MeV/c).

The errors displayed are statistical. Systematic errors in the total reaction cross sections (due mainly to an error in the estimation of the target transparency) are of the order of 3% [2,4]; those for σ_{BU} are about 12% [4]. The R values at 306.2 MeV/c and at 607.7 MeV/c are underestimated by a factor smaller than 4% due to $\bar{p}p \rightarrow \bar{n}n$ charge exchange effects [3].

Tab. III Mean number per event of charged prongs, $\pi^{\pm}$ and heavy particles at four $\bar{p}$ momenta. The data at 306.2 MeV/c include a small background of annihilationless events (see text).

Figure Captions

Fig. 1. Cross sections in mb as defined in caption of Tab. II. $\sigma(\bar{p}p)$ and $\sigma(\bar{p}n)$ correspond to $P(\bar{p}p)$ and $P(\bar{n}p)$.

Fig. 2. Percentages of annihilation events with production of ^3H, ^3He and of particles other than ^3H and ^3He.

Fig. 3. Lower and upper limits for the production of no heavy prong (Oh), p or ^2H. (o) Production of ^3He.
(□) Upper limit for the production of particles other than ^3H and ^3He (The same behaviour is reported in Fig.2).

Fig. 4. Momentum distributions for p, ^2H, ^3H and ^3He. The kinetic energies of the different particles are indicated too. For each particle, the data at different $\bar{p}$ momentum are included in the same histogram.

Fig. 5. Momentum distributions for heavy particles not identified as p, ^2H or ^3H and for positive particles including π^+, p, ^2H and ^3H but not ^3He.

Fig. 6. $(\leq)\pi^{\leq}$ momentum distribution for $\bar{p}$ at rest (500 tracks). $(\ldots)\pi^{\pm}$ momentum distribution for events with production of ^3He (173 tracks). The curve represents the behaviour of the $\pi^{\leq}$ momentum distribution from $\bar{p}n$ annihilation in deuterium at rest [13]; it is normalized in such a way that its maximum is as high as that of the histogram for $\pi^{\leq}$.

Fig. 7. $(-)\pi^-$ momentum distribution for 600 MeV/c $\bar{p}$ (511 tracks). The curve represents the momentum distribution of π^- produced in $\bar{p}p$ annihilation at 700 MeV/c [13]

Fig. 8. Multiplicity distributions at four energies of the total number of charged prongs and of the negative pions. At rest, at 192.8 and 607.7 MeV/c only annihilation events are considered; at 306.2 MeV/c a small number of break-up events is included (see text). Total number of events utilized: at rest, 2677; at 192.8 MeV/c, 612; at 192.8 MeV/c, 1042; at 607.7 MeV/c, 2859.

	Total number of charged prongs	Number of heavy charged prongs	Type of heavy charged particles
(A)	even	1	^3He
	odd		
(B)		1	^3H
(C)		0	-
(D)		1	p, ^2H
(E)		2	(pp),(p^2H)

Tab. I

σ(mb) P(%)	at rest	192.8 MeV/c	306.2 MeV/c	607.7 MeV/c
σ_R		405.6±16.4	293.7±9.1	239.2±5.0
σ_{CE}			6.1	4.7
$\sigma_{BU}(2)$				4.2±1.3
$\sigma_{BU}(3)$				11.3±2.6
σ_a		405.6±16.4	287.6±8.9	219.0±6.0
$\sigma_a(^3He)$		93.2±7.9	58.6±4.1	34.0±1.8
$P(^3He)$	21.0±0.9	23.0±1.9	20.4±1.4	15.5±0.7
P_o	79.0±0.9	77.0±1.9	79.7±1.4	84.5±0.7
$P(\bar{p}p)$	67.6±2.3	61.1±2.6	59.2±2.1	63.8±3.2
$P(\bar{p}n)$	32.4±2.1	38.9±2.6	40.8±2.1	36.2±3.0
$R = \frac{P(\bar{p}n)}{P(\bar{p}p)}$	0.48±0.03	0.64±0.05	0.69±0.04	0.57±0.05
P(2h)	11.3±2.0	15.9±1.8	20.5±3.0	20.7±2.9
$P(^3H)$	43.7±3.2	35.9±4.1	29.6±2.6	27.2±3.1
$\sigma(^3H)$		145.7±17.6	85.0±8.0	59.6±7.0
$P(0,p,^2H)$	35.3±3.3	41.1±4.5	50.0±3.0	57.3±3.2

Tab. II

	at rest	192.8	306.2	607.7
$\langle n_c \rangle$	4.10±0.07	3.98±0.17	4.05±0.13	4.22±0.07
$\langle n_{\pi^-} \rangle$	1.65±0.03	1.59±0.07	1.63±0.06	1.69±0.03
$\langle n_h \rangle$	1.11±0.05	1.16±0.05	1.21±0.06	1.21±0.04
$\langle n_{\pi^+} \rangle$	1.33±0.09	1.23±0.19	1.21±0.16	1.29±0.09

Tab. III

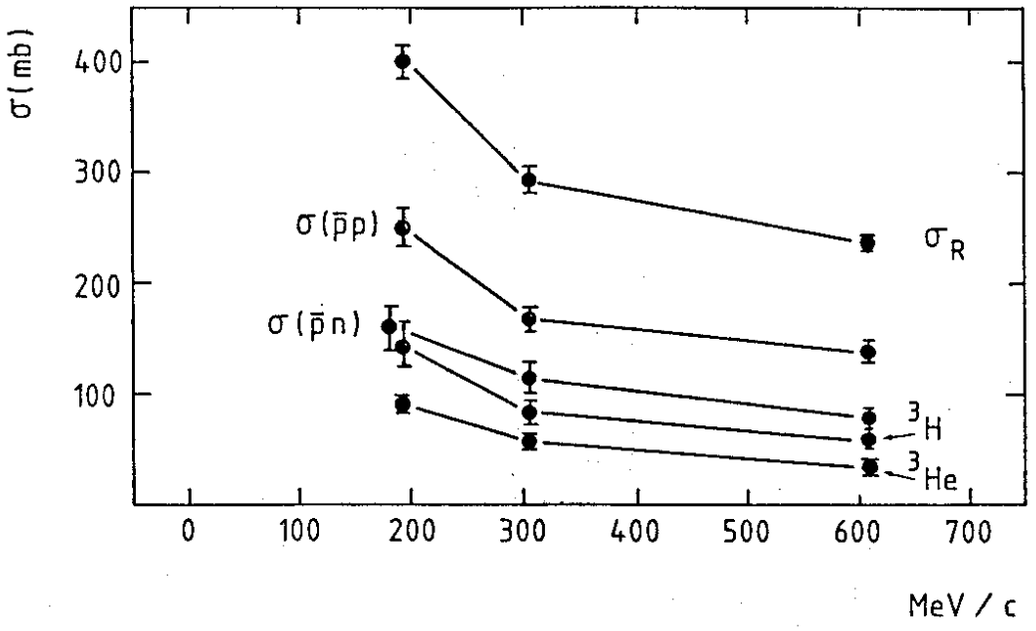

Fig. 1

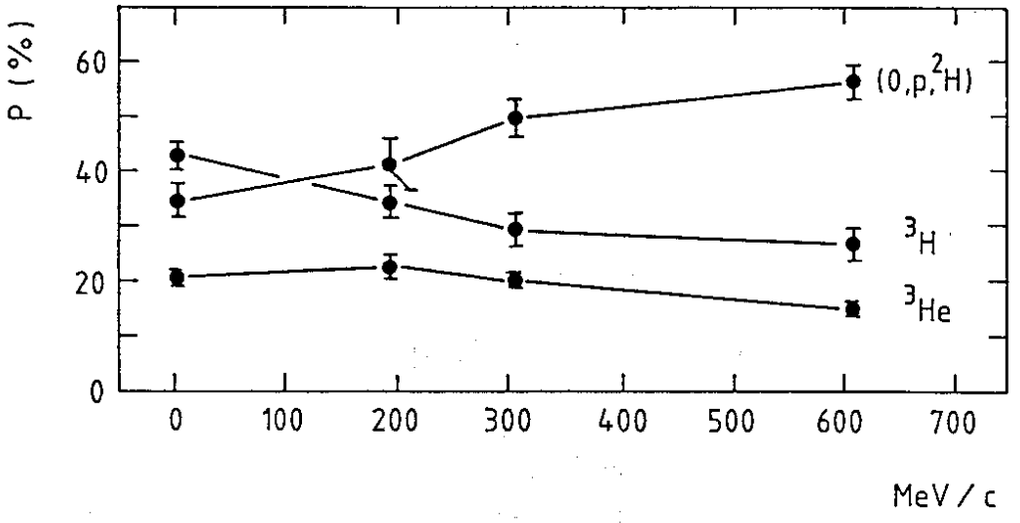

Fig. 2

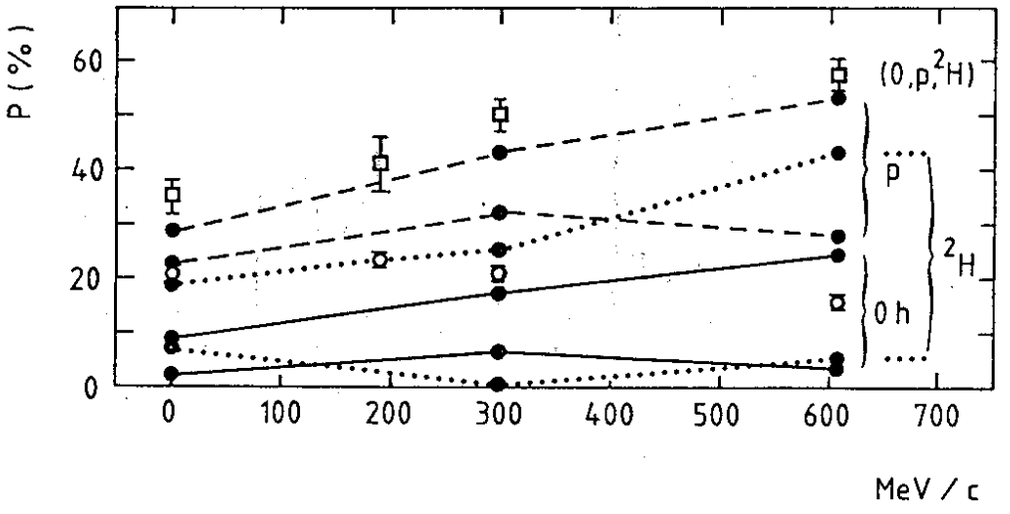

Fig. 3

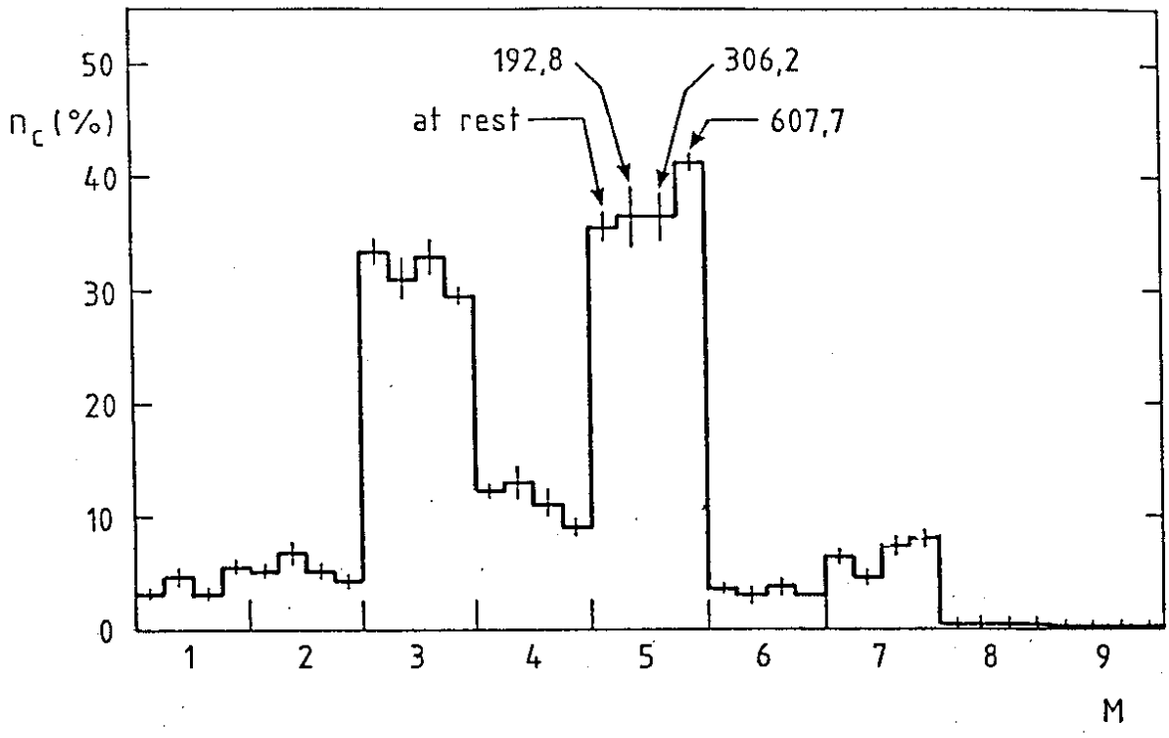
192,8
306,2
at rest
607,7
n_c (%)
50
40
30
20
10
0
1
2
3
4
5
6
7
8
9
M

Fig. 8a

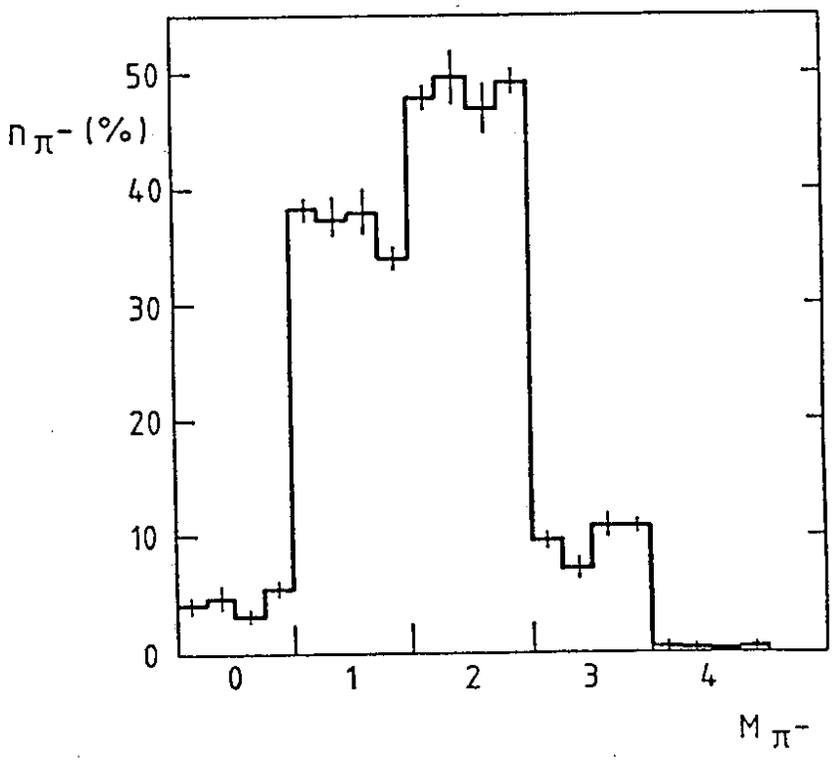
n_{π^-} (%)
50
40
30
20
10
0
0
1
2
3
4
M_{π^-}

Fig. 8b

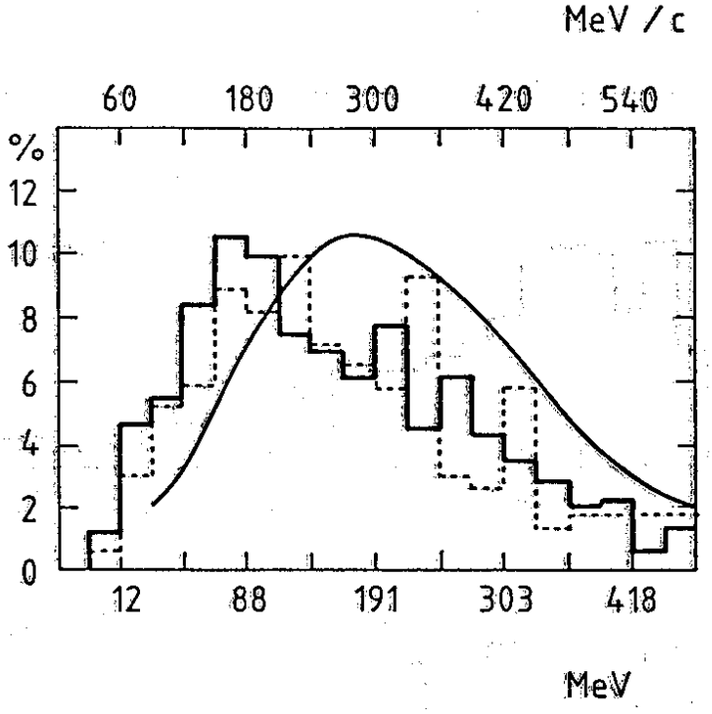
MeV / c
60
180
300
420
540
%
12
10
8
6
4
2
0
12
88
191
303
418
MeV

Fig. 6

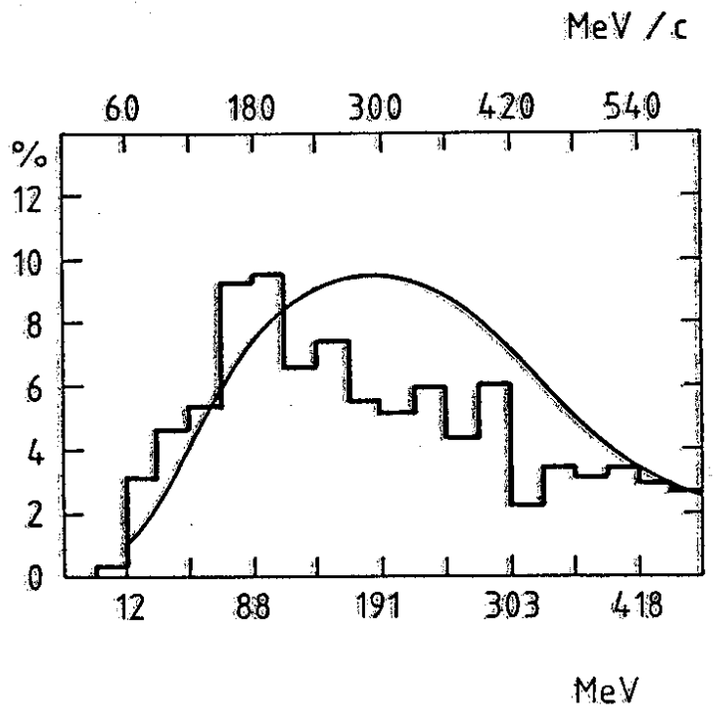
MeV / c
60
180
300
420
540
%
12
10
8
6
4
2
0
12
88
191
303
418
MeV

Fig. 7

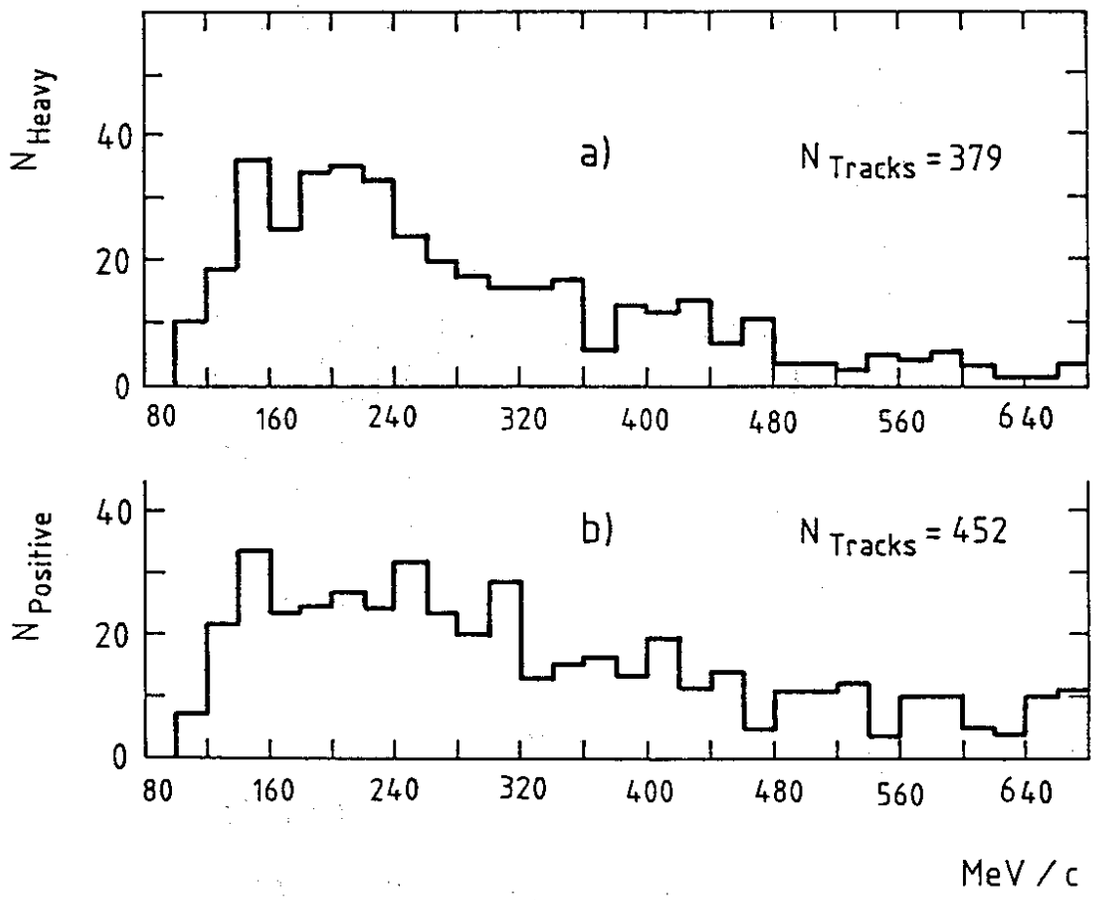
N Heavy
40
20
0
a)
N Tracks = 379
80
160
240
320
400
480
560
640
N Positive
40
20
0
b)
N Tracks = 452
80
160
240
320
400
480
560
640
MeV / c

Fig. 5

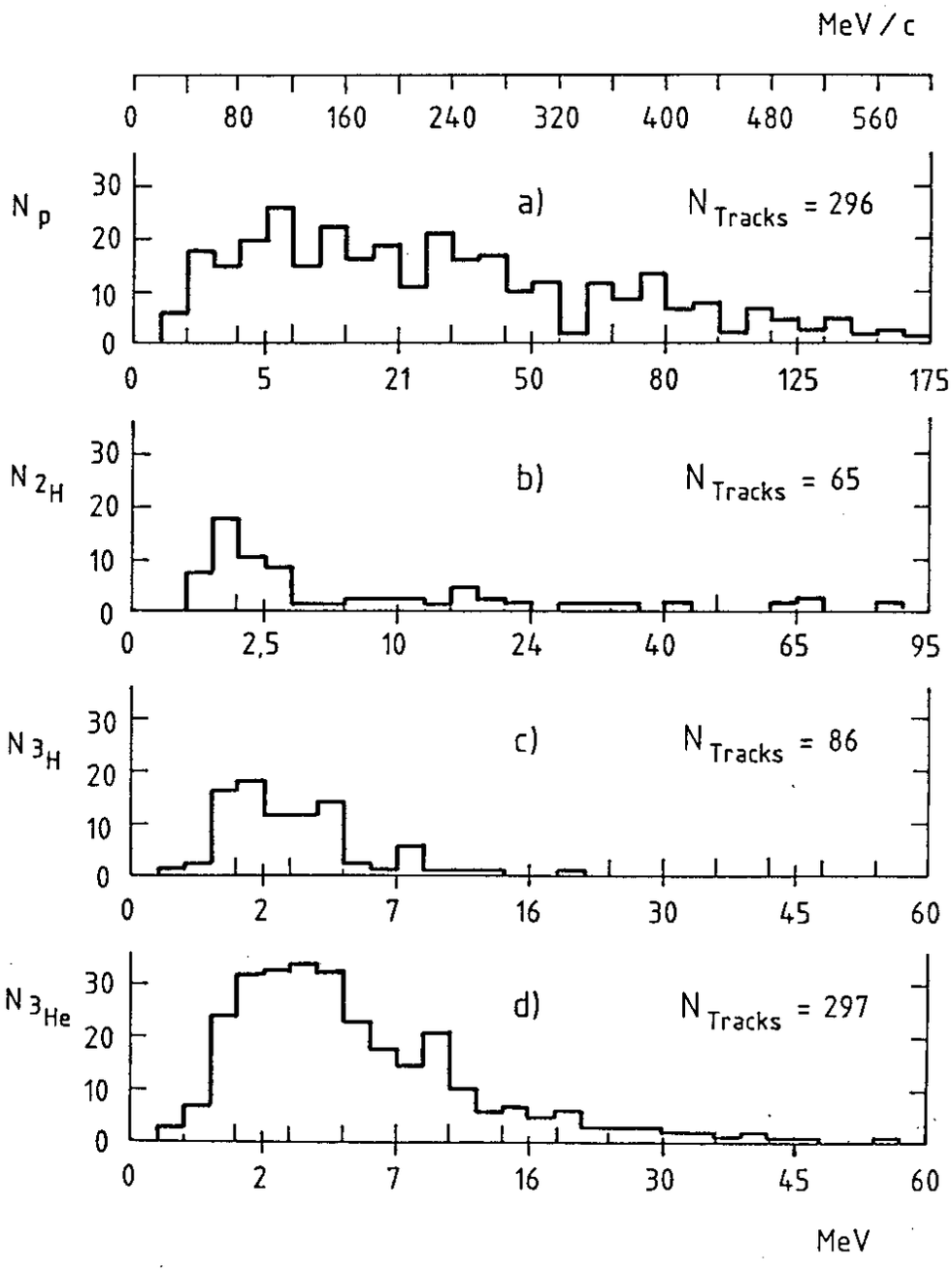
MeV / c
0 80 160 240 320 400 480 560
N p
30
20
10
0
a)
N Tracks = 296
0 5 21 50 80 125 175
N 2H
b)
N Tracks = 65
0 2,5 10 24 40 65 95
N 3H
c)
N Tracks = 86
0 2 7 16 30 45 60
N 3He
d)
N Tracks = 297
0 2 7 16 30 45 60
MeV

Fig. 4